Original Article

MOLECULAR METABOLISM

Pioneer factor Foxa2 enables ligand-dependent activation of type II nuclear receptors FXR and LXRα

Jessica Kain [1], Xiaolong Wei [1], Nihal A. Reddy, Andrew J. Price, Claire Woods, Irina M. Bochkis*

ABSTRACT

Objective: Type II nuclear hormone receptors, including farnesoid X receptors (FXR), liver X receptors (LXR), and peroxisome proliferator-activated receptors (PPAR), which serve as drug targets for metabolic diseases, are permanently positioned in the nucleus and thought to be bound to DNA regardless of the ligand status. However, recent genome-wide location analysis showed that LXRα and PPARα binding in the liver is largely ligand-dependent. We hypothesized that pioneer factor Foxa2 evicts nucleosomes to enable ligand-dependent binding of type II nuclear receptors and performed genome-wide studies to test this hypothesis.

Methods: ATAC-Seq was used to profile chromatin accessibility; ChIP-Seq was performed to assess transcription factors (Foxa2, FXR, LXRα, and PPARα) binding; and RNA-Seq analysis determined differentially expressed genes in wildtype and *Foxa2* mutants treated with a ligand (GW4064 for FXR, GW3965, and T09 for LXRα).

Results: We reveal that chromatin accessibility, FXR binding, LXRα occupancy, and ligand-responsive activation of gene expression by FXR and LXRα require Foxa2. Unexpectedly, Foxa2 occupancy is drastically increased when either receptor, FXR or LXRα, is bound by an agonist. In addition, co-immunoprecipitation experiments demonstrate that Foxa2 interacts with either receptor in a ligand-dependent manner, suggesting that Foxa2 and the receptor, bind DNA as an interdependent complex during ligand activation. Furthermore, PPARα binding is induced in *Foxa2* mutants treated with FXR and LXR ligands, leading to the activation of PPARα targets.

Conclusions: Our model requires pioneering activity for ligand activation that challenges the existing ligand-independent binding mechanism. We also demonstrate that Foxa2 is required to achieve activation of the proper receptor — one that binds the added ligand — by repressing the activity of a competing receptor.

Keywords Lipid metabolism; Liver; Nuclear receptor; Pioneer factor; Foxa2; FXR; LXR

1. INTRODUCTION

Members of the nuclear receptor superfamily; farnesoid X receptors (FXR), liver X receptors (LXR), and peroxisome proliferator-activated receptors (PPAR), function in bile acid, fatty acid, cholesterol, and glucose metabolism [1]. Ligands that activate or antagonize these receptors have been developed to treat metabolic diseases, cardiovascular symptoms, and cancer [2–5]. Nuclear receptors (NR) are classified according to their subcellular localization in the absence of ligand and mechanism of action. Type I receptors, including estrogen (ER) and androgen (AR) receptors, are positioned in the cytoplasm and bound to chaperone heat-shock proteins translocating to the nucleus and binding hormone-response DNA elements — as homodimers on ligand binding. In contrast, type II receptors, such as FXR, LXR, and PPAR, are permanently positioned in the nucleus regardless of the ligand status. They bind DNA as heterodimers in complex with retinoid X receptor (RXR). The accepted paradigm with regard to ligand activation of type II receptors is a two-step process: 1) the receptor is bound to DNA in complex with a co-repressor in the absence of the ligand; 2) binding of the ligand induces a conformational change, co-repressor/co-activator exchange, and initiation of transcription (Figure 1A). However, recent genome-wide location analysis showed that, as in type I receptors ER and AR [6,7], LXRα and PPARα binding in the liver after chronic stimulation is largely ligand-dependent [8]. While binding of ER and AR in a ligand-dependent manner is compatible with their mechanism of action (translocation from the cytoplasm to the nucleus and DNA binding upon ligand binding), a similar process that governs the recruitment of type II receptors, which are permanently nuclear, is unexplained.

We hypothesized that pioneer factor Foxa2 modulates chromatin accessibility by evicting nucleosomes to enable binding by type II

Department of Pharmacology, University of Virginia, Charlottesville, VA, 22908, USA

[1] Jessica Kain and Xiaolong Wei contributed equally to this work.

*Corresponding author. Department of Pharmacology University of Virginia School of Medicine, 5026 Pinn Hall, 1340 Jefferson Park Ave, Charlottesville, VA, 22908. Fax: +434 982 3878. E-mail: imb3q@virginia.edu (I.M. Bochkis).

Received April 1, 2021 • Revision received July 5, 2021 • Accepted July 6, 2021 • Available online 8 July 2021

https://doi.org/10.1016/j.molmet.2021.101291

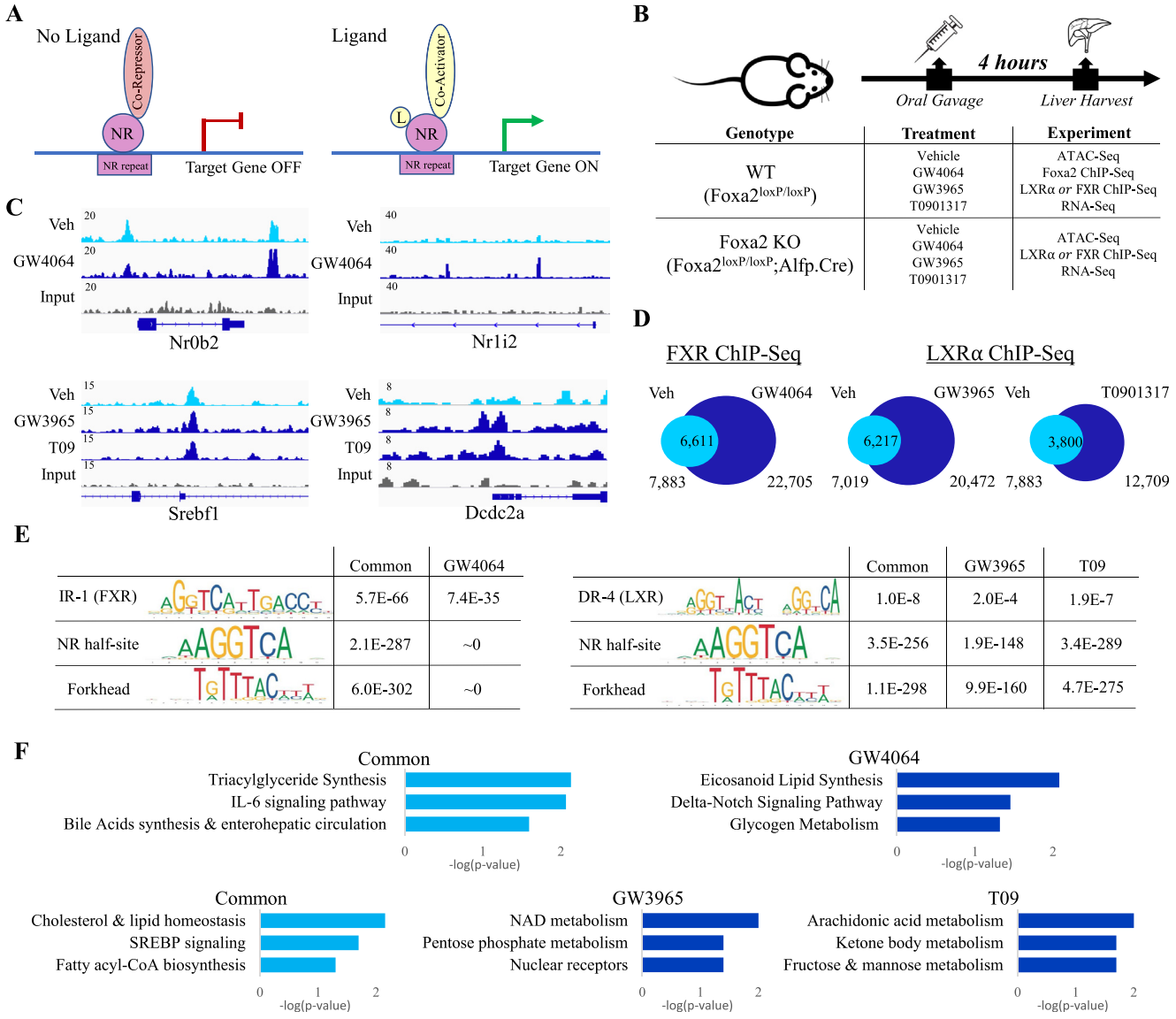

Figure 1: Binding of FXR and LXRα is induced by acute activation. (A) The accepted paradigm regarding ligand activation of type II nuclear receptors (NR) is a two-step process: 1) the receptor as a heterodimer with retinoid X receptor (RXR) is bound to the DNA in complex with a co-repressor in the absence of the ligand; 2) binding of the ligand induces a conformational change, co-repressor/co-activator exchange, and initiation of transcription. (B) Experimental design showing the mice (both WT and *Foxa2* mutants) were treated with an agonist (GW4064 for FXR, GW3965, specific for LXR, or T0901317, which binds LXR and few other related receptors) using oral gavage; Livers were harvested after 4 h of treatment and used for ATAC-Seq, ChIP-Seq (Foxa2, FXR, LXRα), and RNA-Seq experiments. (C) ChIP-seq track view in Integrative Genomics Viewer (IGV) of common (left) and ligand-dependent (right) sites for FXR (top panel, Nr0b2 chr4:133,551,376—133,558,686, Nr1i2 chr16:38,266,836—38,296,668) and LXRα (bottom panel, Srebf1 chr11:60,207,979—60,213,098, Dcdc2a chr13:25,054,003—25,056,498). (D) Venn diagrams showing increased FXR and LXRα binding with acute ligand activation (FXR 7,883 regions for vehicle, 22,705 regions for GW4064, PeakSeq, FDR < 5%, q-value < 0.015 vs Input control; LXRα 7,019 regions for vehicle, 20,472 regions for GW3965 and 12,669 regions for T09, PeakSeq, FDR < 10%, q-value < 0.05, vs. Input control). (E) Scanning motif of positional weight matrices in Jaspar and TRANSFAC databases in FXR (left) and LXRα (right) bound regions. PscanChIP identified highly enriched consensus sites for FXR (IR-1 element) in FXR bound regions and LXR (DR-4 element) in LXRα sites for both common and ligand-dependent targets. Consensus for nuclear receptor half-site and *forkhead* motif was highly enriched in both FXR and LXRα sites. (F) EnrichR analysis of bound regions mapped the sites to closest genes and reported overrepresented pathways, including "triacylglyceride synthesis" and "bile acid synthesis" among common FXR targets and "cholesterol and lipid homeostasis" and "SREBP signaling" among common LXRα targets. Different pathways were enriched among ligand-dependent targets, including "glycogen metabolism", "NAD metabolism", and "ketone body metabolism" (GW4064, GW3965, T09).

nuclear receptors upon ligand activation. Foxa2 is a member of the Foxa subfamily of winged-helix/*forkhead* box (Fox) transcription factors [9], named "pioneer" factors, for their ability to independently bind highly condensed chromatin by displacing linker histones and facilitating access for subsequent binding of additional transcription factors [10]. Foxa2 binds nucleosomal DNA *in vivo* [11] and enables nucleosomal depletion during differentiation [12]. We have previously determined that ligand-responsive activation of FXR gene expression with cholic acid is Foxa2-dependent [13]. As the deletion of Foxa2 in the liver leads to mild cholestasis [14], we placed Foxa2-deficient mice on a diet enriched with primary bile acid cholic acid for seven days. Chronic treatment with cholic acid, an FXR agonist, induced expression of over 7,000 genes in wild-type mice, and more than 2,500 of them were downregulated in *Foxa2* mutants. In addition, we reported that Foxa2 cooperates with ligand-activated PPARα receptors [15] in an aged liver, leading to the development of steatosis.

A previous study has shown that during chronic activation (14 daily ligand injections), the binding of type II nuclear receptors LXRα and PPARα in the liver is largely ligand-dependent [8]. In addition, we established that chronic activation of FXR-dependent gene expression (0.5% cholic acid diet, 7 days) requires Foxa2. In this study, we test the hypothesis that binding of type II nuclear receptors is ligand-dependent during acute activation and requires Foxa2. We demonstrate that chromatin accessibility, recruitment of FXR and LXRα to genomic sites, and FXR-dependent and LXRα-dependent gene expression on ligand binding (using GW4064 for FXR and two ligands, GW3965, and T0901317, for LXR), assayed 4 h after ligand injection, require Foxa2. Unexpectedly, we observed that Foxa2 occupancy is drastically increased when either FXR or LXRα is activated by an agonist. Foxa2 can open closed chromatin, while the agonist does not interact with Foxa2, but binds the ligand-binding domain of the nuclear receptor. Thus, our results suggest that Foxa2 and the receptor, bind DNA as an interdependent complex during ligand activation. Our model that requires pioneering activity for ligand activation of type II nuclear receptors challenges the existing ligand-independent binding mechanism.

Furthermore, we observe that PPARα binding is induced in *Foxa2* mutants treated with FXR and LXR ligands, leading to the activation of PPARα targets. Hence, in addition to its essential role in the activation of ligand-dependent gene expression by type II nuclear receptors — by opening chromatin for ligand-dependent sites — Foxa2 is required to achieve activation of the proper receptor; one that binds the added ligand, by repressing the activity of a competing receptor.

2. MATERIALS AND METHODS

2.1. Animal experimentation

Foxa2 mutant mice were kindly provided by Klaus Kaestner (University of Pennsylvania). The derivation of the $Foxa2^{loxP/loxP}$;Alfp.Cre mouse model has been reported previously [16]. Mice were genotyped by PCR of tail DNA as described [16]. Male mice, 8—12 weeks of age, were used for all studies. For ligand activation studies, mice were treated once with an agonist (GW4064 for FXR, GW3965, and T0901317 for LXRα) using oral gavage. Control mice were treated with vehicle (20 mL propylene glycol/5 mL Tween 80 solution). Agonists were added to the vehicle for experimental treatment. Mice on control treatment were dosed with a volume of 2 mL/kg body weight using oral gavage. Mice on experimental treatment were given a 30 mg/kg dose. Using 15 mg/mL dosing solution, each mouse was administered a volume of 2 mL/kg body weight. Animals on both control and experimental treatments were sacrificed 4 h after gavage. All animal work was approved by Animal Care and Use Committee at UVa (protocol number 4162—03—20).

2.2. ATAC-seq

Nuclei were isolated from frozen liver tissue (50 mg), homogenized in PBS with complete protease inhibitor (PI, Roche) using a glass Dounce homogenizer. The homogenate was collected into a 1.5 mL Eppendorf tube and washed with PBS + PI (2000 g for 3 min at 4 °C). The pellet was resuspended in a 1 mL lysis buffer (10% NP-40, 10% Tween-20, 1% Digitonin) + PI and homogenized. The homogenate was transferred to a 1.5 mL Eppendorf tube and placed on a rotator for 5 min at 4 °C. After centrifugation (2000 g for 5 min at 4 °C), the pellet was washed once with resuspension buffer (1 M Tris—HCl (pH 7.5), 5 M NaCl, 1 M MgCl2, 0.1% tween-20) and centrifuged (2000×*g* for 5 min at 4 °C). The resulting pellet was resuspended in PBS and filtered through a cell strainer (40 μm). The nuclei were counted using the Nexcelom cell counter. Approximately 50,000 nuclei were subsequently used in the tagmentation and library preparation protocol as described [17]. Mitochondrial DNA contamination in amplified libraries was checked by QPCR before sequencing. All samples were sequenced on Illumina NextSeq 500.

2.3. Chromatin immunoprecipitation (ChIP) and ChIP-Seq

Snap-frozen mouse liver (100 mg) from wild-type and *Foxa2* mutant mice treated with vehicle, FXR, and LXR ligands were used to prepare chromatin. ChIP and ChIP-Seq were performed as described previously [18,19]. Foxa2-specific rabbit antiserum (Seven Hills Bioreagents, WRAB-1,200), mouse monoclonal antibody specific to FXR (Cell Signaling, mAb #72105), mouse monoclonal antibody specific to LXRα (R&D Biosystems, PP-PPZ0412-00), and rabbit polyclonal antibody specific to PPARα (Novus Biologicals, NB600-636) were used for immunoprecipitation. All samples were sequenced on Illumina NextSeq 500.

2.4. Co-immunoprecipitation (Co-IP) and Western blotting (WB)

Mouse liver tissue was washed with cold PBS and then lysed by homogenizing in cell lysis buffer (Cell Signaling Technology). After centrifugation at 14,000 rpm for 15 min at 4 °C, the supernatants were collected, and the protein concentrations were measured using BCA protein assay reagents (Thermo Fisher). Subsequently, Co-IP was performed according to the immunoprecipitation protocol (Thermo Fisher) (thermo_sher.com/immunoprecipitation). Briefly, antibodies were added to the protein G Dynabeads, incubated with rotation for 10 min at room temperature for binding. The beads—antibody complex was then crosslinked using the crosslinking reagent BS3 at room temperature for 30 min. After washing to remove non crosslinked antibodies, the antibody-crosslinked beads were incubated with equal amounts of protein lysates overnight in a cool room. The beads were washed 5 times with 500 μL of IP cell lysis buffer and then eluted using 50 mM glycine. The eluted proteins were separated in Bolt 4—12% Bis-Tris gradient gel (Invitrogen) and transferred onto PVDF membranes (Azure). After blocking with 5% milk, the membranes were probed at 4 °C overnight with various primary antibodies: anti-Foxa2 (Seven Hills, WRAB-1200), FXR (Cell Signaling, mAb #72105), LXR-α (Abcam, ab41902), and histone H3 (Millipore, 04—928) washed with TBST (20 mM Tris, 150 mM NaCl, 0.1% Tween 20; pH 7.6), and incubated with horseradish peroxidase (HRP)-conjugated secondary antibodies (Promega) at room temperature for 1 h. Finally, after washing with TBST, the antibody-bound membranes were treated with enhanced chemiluminescent Western blot detection.

2.5. RNA isolation and sequencing

Liver RNA was isolated from $Foxa2^{loxP/loxP}$, Alfp.Cre mice, and control littermates as described previously [16]. The quality of RNA samples was analyzed using Agilent RNA 6000 Nano Kit (Bioanalyzer, Agilent Technologies). Samples with RIN scores above 9.5 were used in library preparation. Approximately 1 μg of total RNA was used to isolate mRNA (NebNext Poly(A) mRNA Magnetic Isolation Module). Libraries of resulting mRNA were prepared using the NebNext Ultra II RNA library preparation kit. All samples were sequenced on Illumina NextSeq 500.

2.6. ATAC-seq analysis

Paired-end reads were aligned to the mouse genome (mm10; NCBI Build) using BWA [20]. Duplicate reads were removed. Reads (Phred score > 30) that aligned uniquely were used for subsequent analysis. Data from two biological replicates were merged for each condition (WT Veh, WT GW4064, WT GW3965, WT T09, Foxa2 KO Veh, Foxa2 KO

GW4064, Foxa2 KO GW3965, Foxa2 KO T09). PeakSeq [21] was used to identify chromatin accessibility in the ligand-activated condition against vehicle controls (WT GW4064 vs. WT Veh, WT GW3965 vs. WT Veh, WT T09 vs. WT Veh, FDR 5%, q-value < 0.05).

2.7. ChIP-seq analysis

Reads were aligned to the mouse genome (mm10; NCBI Build) using BWA [20]. Duplicate reads were removed. Reads (Phred score > 30) that aligned uniquely were used for subsequent analysis. For Foxa2 ChIPs, data from three biological replicates were merged for each condition (WT Veh, WT GW3965, WT T09) and two biological replicates were merged for WT GW4064. For FXR ChIPs, data from two biological replicates were merged for each condition (WT Veh, WT GW4064, Foxa2 KO Veh, Foxa2 KO GW4064). For LXRα ChIPs, data from four biological replicates were merged for each condition (WT Veh, WT GW3965, WT T09, Foxa2 KO Veh, Foxa2 KO GW3965, Foxa2 KO T09). For PPARα ChIP, data from two biological replicates were merged for each condition (WT Veh, WT4064, WT GW3965, WT T09, Foxa2 KO Veh, Foxa2 KO GW4064, Foxa2 KO GW3965, Foxa2 KO T09). PeakSeq [21] was used to identify bound peaks in FXR ligand-activated condition against input controls (Foxa2 FDR 5%, q-value < 0.01; FXR FDR 5%, q-value < 0.015; PPARα FDR 5, q-value<0.07) and in LXR ligand-activated condition against input controls (Foxa2 FDR 5%, q-value < 0.0005; LXRα FDR 10%, q-value < 0.05; PPARα FDR 5%, q-value<0.07). Q-values were adapted empirically based on coverage and ChIP results for each antibody.

2.8. RNA-seq analysis

RNA-Seq reads were aligned using STAR [22] to mouse genome build mm10. Expression levels were calculated using RSEM [23]. Differential expression analysis of RNA-seq (p-value <0.05) was performed in R using the EdgeR package [24] with a Benjamini—Hochberg FDR of 5%. Four replicates were sequenced for each condition. Outliers were identified and removed using principal component analysis (PCA). Three replicates were used for WT Veh, WT GW4064, Foxa2 KO Veh, Foxa2 KO GW4064, WT GW3965, WT T09, and Foxa2 KO T09. Four replicates were used for WT Veh, Foxa2 KO Veh, and Foxa2 KO GW.

2.9. Functional analysis

Ingenuity Pathway Analysis (IPA) curates information gathered from the literature and genomic experiments (microarray, RNA-Seq, ChIP-Seq) to determine sets of targets controlled by a regulator (a transcription factor, chromatin remodeler, kinase, and small molecule) and the logic of this regulation (activation or repression). IPA compares the overlap of each such set of targets with the subset of genes that are controlled by each regulator in an experimental gene list and reports the p-value of the overlap (Fisher's exact test). If the overlap is significant, and the expression changes agree with those expected from the regulatory connection (e.g., genes activated by the regulator are activated in the analysis data set and repressed genes are repressed), IPA predicts whether the regulator associated with the gene targets is itself activated or inhibited. Analysis of overrepresented functional categories and upstream regulators in ingenuity pathway analysis and heat map generation for RNA-Seq data was performed as described [15]. Samtools bedcov was used to quantify the coverage of ATAC-Seq and ChIP-Seq signal on regions called by PeakSeq and to identify overlaps proportional to sequencing depth (coverage $\geq$ 2 reads/bp, except Foxa2 ChIP WT GW4064, coverage $\geq$ 1.5 reads/bp; FXR WT Veh on WT-GW4064, coverage $\geq$ 2.5 reads/bp; LXRα WT Veh on WT GW3965 and WT T09, coverage $\geq$ 2.5 reads/bp). Foxa2 ChIP WT-GW4064 had the lowest coverage (n = 2); hence, we used a lower threshold. In contrast, for comparisons of ChIP samples from the same antibody, a higher threshold was used owing to higher coverage around the called peaks. Heatmaps of ChIP-Seq coverage were generated by deep tools [25]. Chromatin-x enrichment analysis and analyses for overrepresented pathways and disease conditions were performed by Enrichr [26]. Sequence analysis for overrepresented transcription factor binding motifs in regions from ChIP-Seq experiments was performed by PscanChIP [27].

2.10. Data availability

Genomic data from this study (ATAC-Seq, ChIP-Seq, RNA-Seq) can be accessed at GEO accession number GSE149075. Lists of differentially expressed genes for FXR activation and LXRα activation are provided in Supplemental Tables 1 and 2, respectively. Genes associated with gene expression heatmaps are provided in Supplemental Table 3.

3. RESULTS

3.1. Binding of FXR and LXRα is induced by acute activation

A recent genome-wide binding study demonstrated that LXRα and PPARα occupancy in the liver during chronic activation is largely ligand-dependent [8], disputing the accepted ligand-independent binding mechanism depending only on co-factor exchange for ligand activation of type II nuclear receptors (Figure 1A) [1]. Mice were injected with an agonist for 14 consecutive days, drastically changing their physiology. Hence, the binding of nuclear receptors could have responded to compensate for the physical alterations in a feedback loop. In contrast, we tested the hypothesis that nuclear receptor occupancy is ligand-dependent during acute activation, before physiological changes. We focused on two factors: farnesoid X receptor (FXR), the main regulator of bile acid metabolism; and closely related liver X receptor (LXR), an important regulator of cholesterol homeostasis. We treated the mice once with an agonist (GW4064 for FXR, GW3965, specific for LXR, or T0901317, which binds LXR and few other related receptors) using oral gavage and harvested the livers after 4 h of treatment (experimental design in Figure 1B). Then, we performed FXR and LXRα genome-wide location analysis to assess acute changes in NR occupancy in the livers of mice treated with the ligand. Ligand-independent sites were found at *Nr0b2* and *Srebf1* loci, known targets of FXR and LXRα, respectively [28,29] (Figure 1C, left panel). We further characterized classical FXR (*Nr0b2* & Ostb/*Slc51b*) and LXRα (*Srebf1* & *Abca1*) targets, demonstrating that FXR & LXRα binding at these loci is ligand-independent (Supplemental Figures. 1A and B). Ligand-dependent sites were detected at *Nr1i2* locus for FXR and *Dcdc2a* for LXRα (Figure 1C, right panel). Overall, we observed that both FXR and LXRα binding greatly increases during ligand activation (FXR 7,883 regions for vehicle, 22,705 regions for GW4064; LXRα 7,019 regions for vehicle, 20,472 regions for GW3965, and 12,669 regions for T09, Figure 1D). Scanning motif of positional weight matrices in Jaspar and TRANSFAC databases by PscanChIP identified highly enriched consensus sites — for FXR (IR-1 element) in FXR bound regions and LXR (DR-4 element) in LXRα sites — for both common and ligand-dependent targets. Consensus for nuclear receptor half-site and *forkhead* motif was highly enriched in all FXR and LXRα sites (Figure 1E). EnrichR analysis of bound regions mapped the sites to closest genes and reported overrepresented pathways, including "triacylglyceride synthesis" and "bile acid synthesis" among common FXR targets and "cholesterol and lipid homeostasis" and "SREBP signaling" among common LXRα targets (Figure 1F). Different pathways were enriched among ligand-dependent targets, including "glycogen metabolism", "NAD metabolism", and "ketone

body metabolism" (GW4064, GW3965, T09). The presence of highly enriched motifs (IR-1 for FXR and DR-4 for LXR) and overrepresented pathways associated with known targets of these receptors demonstrate the quality of our binding results.

3.2. Chromatin accessibility increases with the addition of FXR and LXR ligands

Next, we hypothesized that an increase in chromatin accessibility leads to additional nuclear receptor binding during ligand activation (Figure 2A) and profiled chromatin accessibility in livers of mice treated with FXR and LXR ligands (ATAC-Seq). For classical FXR (*Nr0b2* and Ostb/*Slc51b*) and LXRα (*Srebf1* and *Abca1*), chromatin accessibility does not change with agonist corresponding to ligand-independent binding (Supplemental Figure 1B). In contrast, the addition of the agonist leads to significant chromatin opening at the loci of FXR target Cyp3a11, LXR target Scd1, and Lpin1 (Figure 2B), in a genome-wide manner (GW4064, 60,528 regions, left panel; GW3965, 59,054 regions, middle panel; and T09, 59,783 regions, right panel, Figure 2C). The overlap analysis between increased chromatin accessibility and ligand-dependent binding of nuclear receptors determined 18,071 regions for GW4064, 11,097 for GW3965, and 10,717 for T09 (Figure 2C), which confirmed that additional receptor binding during ligand activation occurs at newly opened chromatin sites.

In addition to using our binding data, we took advantage of published ChIP-Seq data sets in the mouse genome and performed an additional overlap analysis between regions of ligand-dependent chromatin and the binding data present in the ChEA database (Supplemental Figure 2A, ChEA analysis in EnrichR [26]). Regions of increased accessibility for both FXR and LXRα activation were enriched for known binding sites of nuclear receptors LXR, RXR, PPARα, PPARγ, and *forkhead* factor FOXO1. FXR ChIP-Seq data are not available in the ChEA database. Our results are consistent with a previous finding that LXR binding sites are extensively shared with other nuclear receptors in the liver [8]. Scanning motif of positional weight matrices in Jaspar and TRANSFAC databases in regions of newly opened chromatin during ligand activation by PscanChIP (Figure 2D) [27] identified consensus sites for FXR (IR-1 element, p-value $<$ 4.5E-96) in regions induced by FXR agonist and for LXR (DR-4 element, p-value $<$ 2.4.9E-77 for GW3965, 3.5.9E-67 for T09) in sites induced by LXR ligands. Consensus for nuclear receptor half-site and *forkhead* motif were found highly enriched in regions induced by ligands for both receptors. Together, these analyses confirm that newly opened chromatin sites are bound by FXR and LXRα and suggest a role for forkhead factors in chromatin opening during ligand activation.

3.3. Foxa2 opens chromatin for FXR and LXRα binding during acute ligand activation

We have previously determined that ligand-responsive activation of FXR gene expression is Foxa2-dependent [13] and that Foxa2 cooperates with ligand-activated PPARα receptors [15] in an aged liver. We hypothesized that pioneer factor Foxa2 modulates chromatin accessibility by evicting nucleosomes to enable type II nuclear receptors' binding upon acute ligand activation (Figure 3A). Hence, we performed ATAC-Seq in livers of *Foxa2* mutants and their control littermates treated with FXR and LXR ligands (*Foxa2*$^{loxP/loxP}$*; Alfp. Cre* described in [16]). For classical FXR (*Nr0b2* & Ostb/*Slc51b*) and LXRα (*Srebf1* & *Abca1*) with ligand-independent binding, chromatin accessibility does not change with the addition of the ligand in wildtype controls and *Foxa2* mutants (Supplemental Figure 1B). Ligand-dependent gene activation of these targets is independent of Foxa2 (Supplemental Figure 1C). In contrast, changes in chromatin accessibility observed at the loci of ligand-dependent FXR and LXR targets *Cyp3a11* (Figure 3B, top panel) and *Scd1* (Figure 3B, bottom panel), and in a genome-wide manner (Figure 3E), are absent in *Foxa2*-deficient livers.

While we detected no ATAC-Seq signal in *Foxa2* mutants at newly opened sites in wildtype controls, there were substantial global changes in chromatin accessibility of these mice at other loci (GW4064, 82,561 regions, left panel; GW3965, 32,694 regions, middle panel; and T09, 66,013 regions, right panel, Figure 2C, Supplemental Figures 2B and C). EnrichR analysis reported "unfolded protein response", "Stat3 signaling', and "mTORC1 Signaling" as significantly enriched pathways in *Foxa2*-deficient mice on ligand treatment, consistent with our previous phenotypic characterization [14,30]. In addition, the "PPAR alpha pathway" and DR-1 element bound by PPAR factors were highly overrepresented in newly opened regions in *Foxa2* mutants (Supplemental Figures 2D and E).

Next, we performed genome-wide location analysis of Foxa2 in wildtype controls treated with FXR and LXR agonists and observed that additional Foxa2 binding sites at the *Cyp3a11* locus in livers treated with FXR agonist GW4064 and at the *Scd1* locus in livers treated with LXR ligand GW3965 correspond to an increase in chromatin accessibility that is absent in *Foxa2* mutants (Figure 3B). Unexpectedly, Foxa2 occupancy dramatically increased with the addition of either ligand (7,306 for vehicle, 22,666 for GW4064; 4,348 regions for vehicle, 21,245 regions for GW3965, 25,318 regions for T09, Figure 3C). Because protein levels of Foxa2 did not change either with FXR or LXR activation (Figure 3D), an increase in Foxa2 binding upon agonist addition is independent of Foxa2 expression.

Then, we proceeded to ascertain the overlap of open regions induced by FXR and LXR ligands in controls and absent in *Foxa2* mutants with additional Foxa2 binding, computing the intersection using Foxa2 ChIP-Seq coverage at ATAC-Seq regions. We found that 23,632, 20,504, and 24,455 (GW4064, GW3965, and T09, respectively) regions with induced chromatin accessibility were bound by Foxa2. The number of Foxa2 occupied regions in the overlap is comparable or exceeds the number of Foxa2 sites that were known as bound during ligand activation by PeakSeq at our chosen cutoff for the respective FXR and LXR experiments (Figure 3E). We observed a dramatic change in Foxa2 occupancy in livers treated with FXR and LXR agonists.

3.4. Foxa2 interacts with FXR and LXRα in a ligand-dependent manner

Foxa2 is not known to bind nuclear receptor agonists directly and has no ligand-binding domain. Considering that Foxa2 opens closed chromatin and the agonist does not interact with Foxa2 but binds the ligand-binding domain of the nuclear receptor, we hypothesized that Foxa2 and nuclear receptor binding to DNA is interdependent (Figure 4A). We observed co-localization of Foxa2 and FXR (Figure 4B, left panel) and Foxa2 and LXRα (Figure 4B, right panel) binding upon the addition of the agonist. In addition, the binding of both nuclear receptors at those loci was Foxa2-dependent. To test our hypothesis, we performed immunoprecipitation experiments and determined that Foxa2 and the receptor interact in a ligand-dependent manner. Liver extracts were immunoprecipitated with an antibody to FXR (Figure 4C, left panel) or LXRα (Figure 4C, right panel). Then, subsequent immunoprecipitate was blotted with an antibody to Foxa2, showing a strong interaction between FXR & Foxa2 with GW4064 treatment (Figure 4C, left panel) and LXRα & Foxa2 with both agonists (Figure 4C, right panel), but not in IgG and vehicle controls.

We also demonstrate that Foxa2 and FXR co-localize at regions of GW4064-induced chromatin accessibility (Figure 4D, left panel).

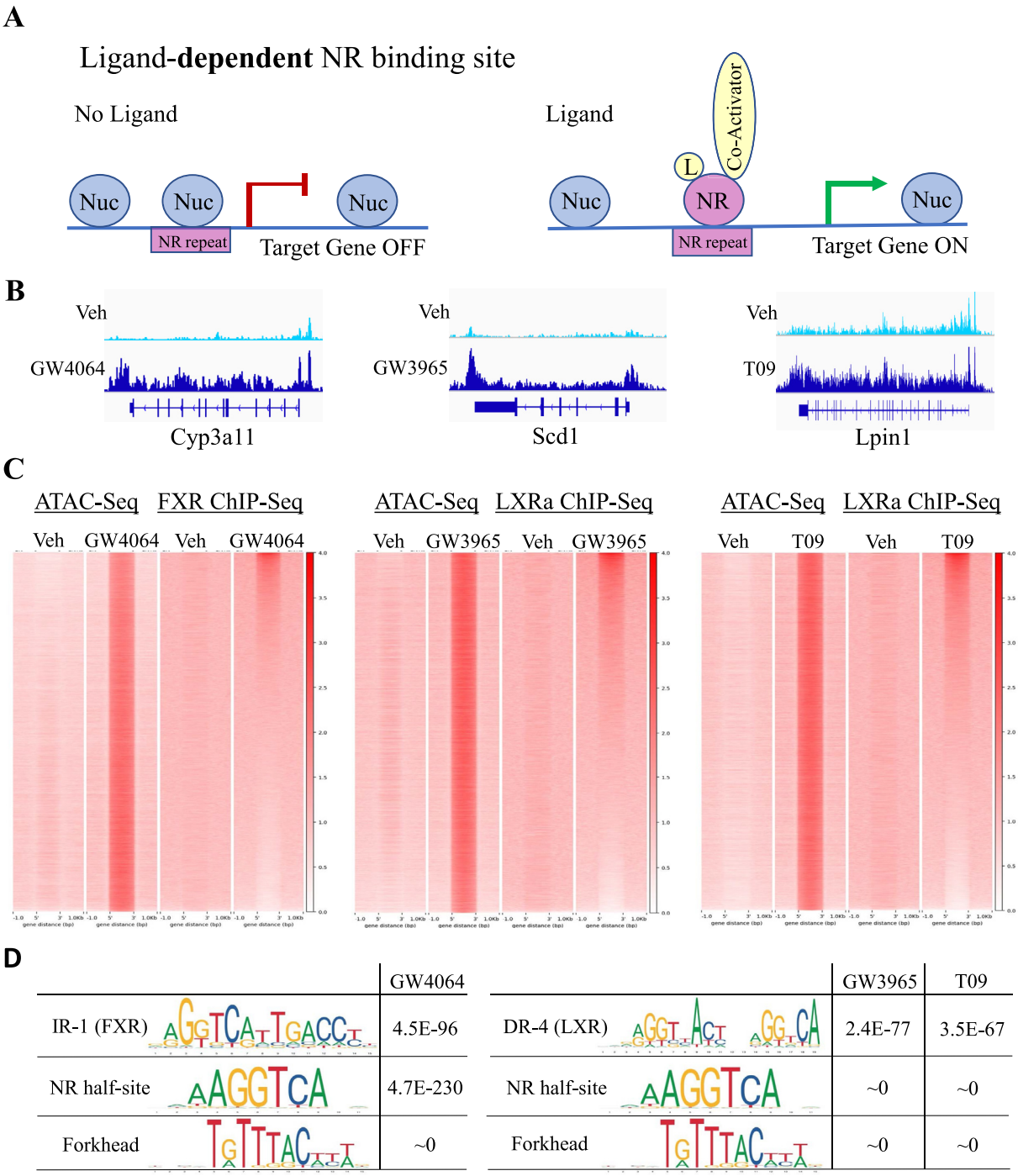

Figure 2: Chromatin accessibility increases with the addition of FXR and LXR ligands. (A) We distinguish between ligand-independent and ligand-dependent nuclear receptor (NR) binding sites. Ligand-independent NR sites are always accessible (Figure 1A). In contrast, ligand-dependent NR sites are inaccessible without ligand activation (occupied by a nucleosome, Nuc, left panel) and become exposed upon stimulation (right panel). (B) ATAC-seq track view in IGV of induced chromatin accessibility with ligand activation (GW4064, Cyp3a11, left panel; GW3965, Scd1 middle panel; T09, Lpin1, right panel). (C) Heatmaps showing a genome-wide increase in ATAC-Seq signal with ligand activation in wildtype controls intersects with additional nuclear receptor binding (FXR and LXRα ChIP-Seq). The overlap analysis between increased chromatin accessibility and ligand-dependent binding of nuclear receptors (2 reads/bp for ChIP-Seq for PeakSeq called ATAC-Seq region, details in methods) determined 18,071 regions for GW4064. 11,097 for GW3965, and 10,717 for T09), confirming that additional receptor binding during ligand activation occurs at newly opened chromatin sites. (D) Scanning motif of positional weight matrices in Jaspar and TRANSFAC databases in regions of newly opened chromatin during acute ligand activation (FXR ligand GW4064 on the left, LXR ligands GW3965 and T09 on the right). PscanChIP identified consensus sites for FXR (IR-1 element, p-value $<$ 4.5E-96) in regions induced by FXR agonist and for LXR (DR-4 element, p-value $<$ 2.4.9E-77 for GW3965, 3.5.9E-67 for T09) in sites induced by LXR ligands. Consensus for nuclear receptor half-site and *forkhead* motif were found highly enriched in regions induced by ligands for both receptors.

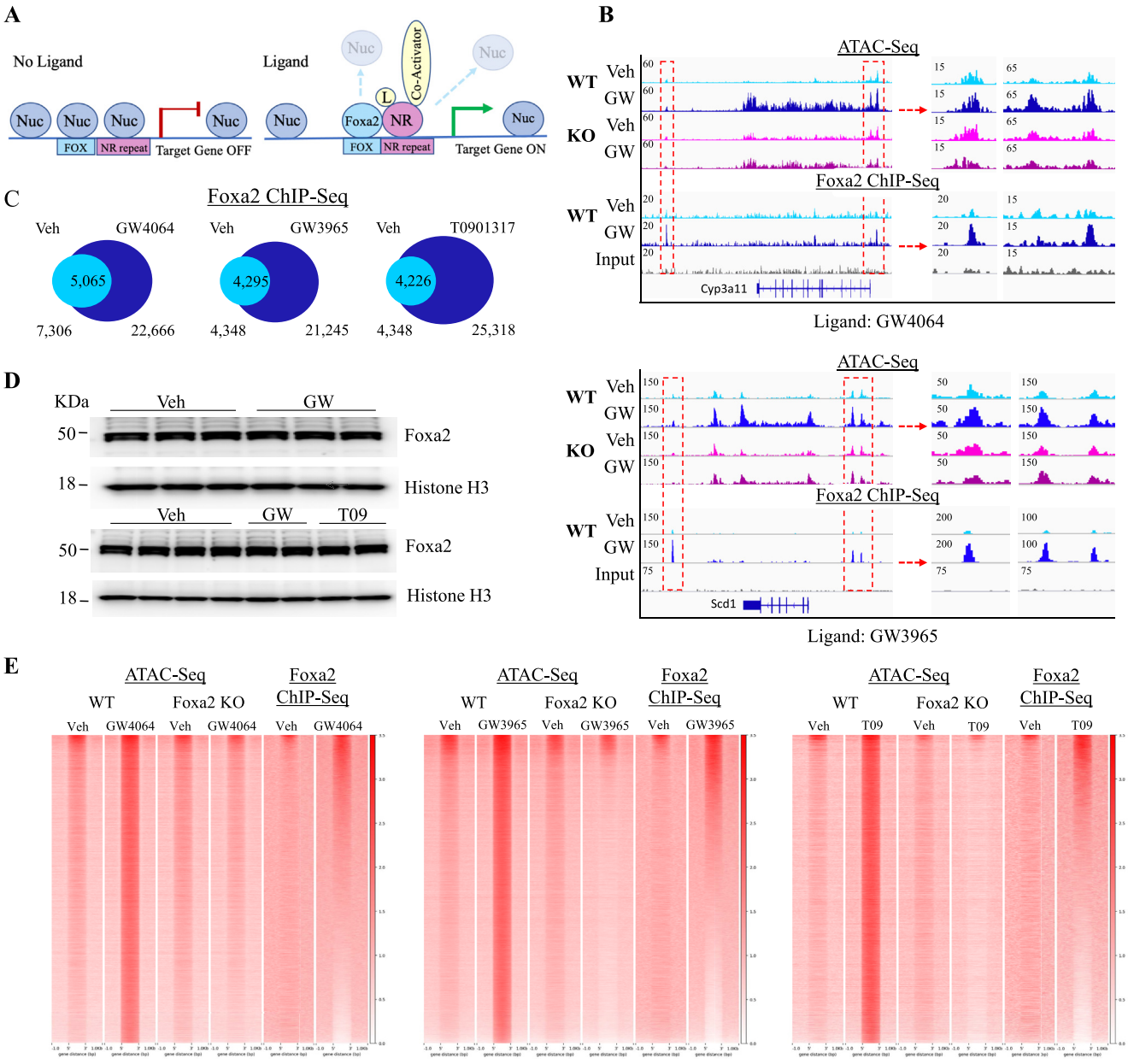

Figure 3: Increase in chromatin accessibility with the addition of FXR and LXR ligands requires Foxa2. (A) We hypothesized that pioneer factor Foxa2 modulates chromatin accessibility by evicting nucleosomes to enable binding by type II nuclear receptors upon acute ligand activation. (B) Ligand-dependent increase in chromatin accessibility correlates to additional Foxa2 binding during GW treatment activation observed at the Cyp3a11 and Scd1 loci, FXR and LXRα targets, respectively (IGV view of Foxa2 ChIP-Seq signal, bottom tracks, track of input reads is provided for comparison.). Middle and right panel (chr5:145,831,500–145,837,794; chr5:145,879,024–145,882,170, top panel, chr19:44,376,869–44,383,515; chr19:44,414,227–44,420,873, bottom panel) are zoomed in regions marked by red rectangles on the left panel. (C) Venn diagrams showing Foxa2 binding is induced by FXR and LXR agonists (7,306 for vehicle, 22,666 for GW4064, PeakSeq, FDR $<$ 5%, q-value $<$ 0.015 vs. Input control; 4,348 regions for vehicle, 21,245 regions for GW3965, 25,318 regions for T09; PeakSeq, FDR $<$ 5%, q-value $<$ 0.0005 vs. Input control) (D) Western blot analysis of protein nuclear extracts from three control livers treated with vehicle and three livers treated with FXR agonist GW4064 (top panel) and four control livers treated with vehicle, two livers treated with LXR agonist GW3965, and two livers treated with LXR agonist T09 with antibodies to FOXA2 and histone H3 (loading control). (E) Heatmaps showing genome-wide increase in ATAC-Seq signal with ligand activation in wildtype controls is absent in *Foxa2*-deficient livers (GW4064, 57,469 regions, left panel; GW3965, 56,630 regions, middle panel; T09, 58,085, right panel; PeakSeq, FDR $<$ 5%, q-value $<$ 0.05; bedcov coverage $\geq$ 2 reads/bp). Overlap of these open regions with additional Foxa2 binding was computed using Foxa2 ChIP-Seq coverage at ATAC-Seq regions (23,632 regions for GW4064, coverage $\geq$ 1.5 reads/bp, 20,504, and 24,455 regions for GW3965 and T09, respectively, 2 reads/bp).

Similarly, Foxa2 and LXRα are found together at sites where chromatin accessibility is increased by LXR agonists GW3965 and T09 (Figure 4D, middle, right panel). In addition, we reveal that ligand-responsive binding of FXR and LXRα is absent in *Foxa2* mutants and is Foxa2-dependent (Figure 4E). In contrast, we also found that FXR and LXRα occupy different regions in Foxa2-deficient livers (FXR: 4,284 regions vehicle, 3,901 regions for GW4064; LXR: 3,214 regions vehicle, 8,803 regions for GW3965, 8,583 regions for T09; Supplemental Figures 3A and B). We detected a slight decrease in FXR expression in *Foxa2* mutants treated with GW4064 that cannot explain a drastic decrease in FXR binding. Protein levels of LXRα did not change in *Foxa2*-deficient livers treated with either ligand

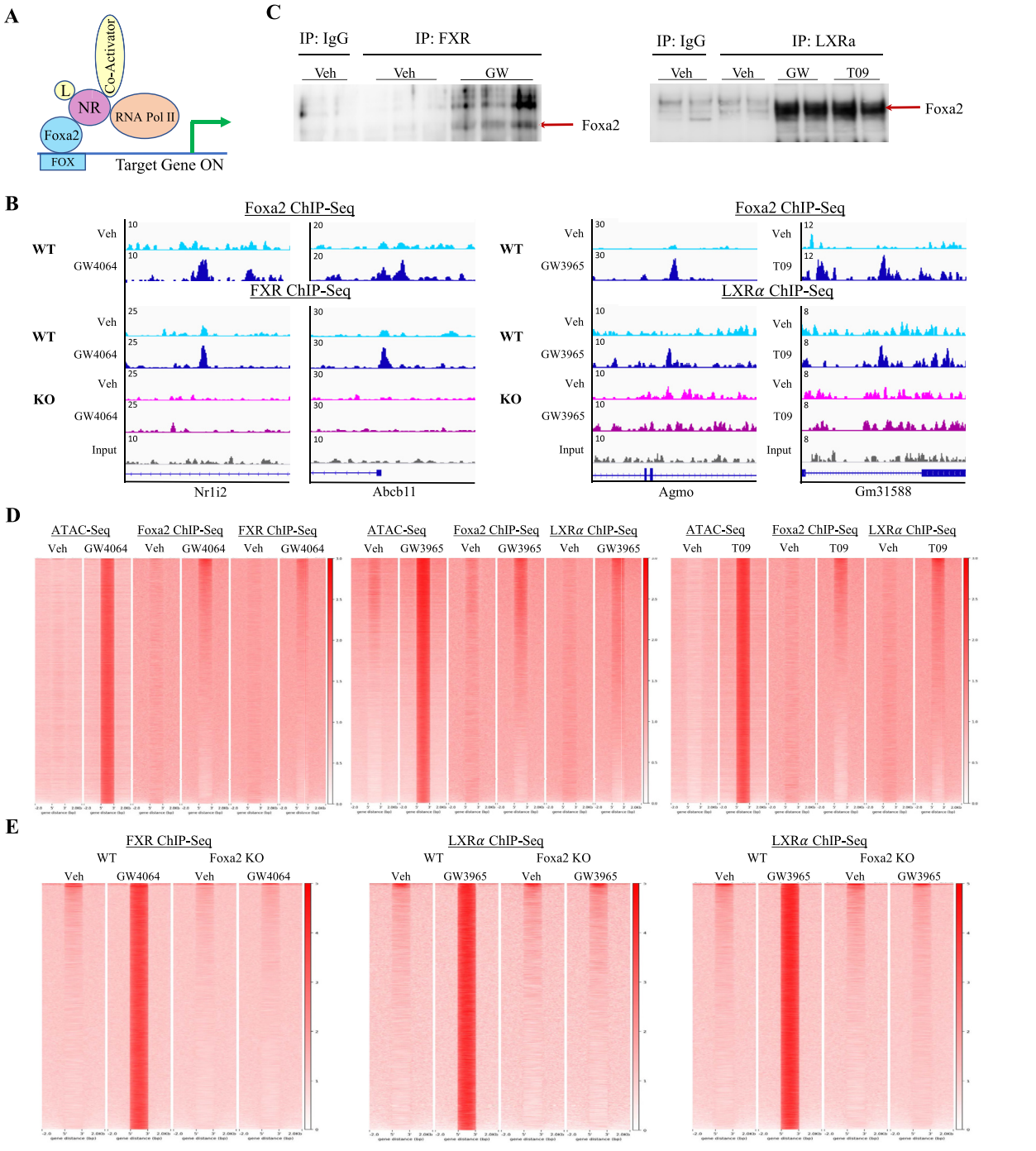

Figure 4: Foxa2 interacts with FXR and LXRα in a ligand-dependent manner. (A) Foxa2/NR interaction model. Foxa2 and liganded nuclear receptor, either FXR or LXRα, form a complex, with pioneer factor binding DNA at the *forkhead* (Fox) binding site. (B) ChIP-seq track view in IGV of colocalized Foxa2 and FXR binding at *Nr1i2* (chr16:38,277,930—38,282,000, left panel) and *Abcb11* (chr2:69,340,945—69,344,719, right panel) loci. FXR binding at these loci is absent in *Foxa2* mutants. ChIP-seq track view in IGV of colocalized Foxa2 and LXR binding at *Agmo* (chr12:37,400,211—37,405,190, left panel) and *Gm31588* (chr9:92,219,475—92,229,805, right panel) loci. LXR binding at these loci is absent in *Foxa2* mutants. (C) Co-immunoprecipitation experiments in livers of mice treated with FXR ligand (left) and LXR agonists (right). Immunoprecipitation with an antibody to FXR and subsequent blotting with an antibody to Foxa2 shows a strong interaction between FXR and Foxa2 with GW4064 treatment, but not in IgG and vehicle controls (left panel). Similarly, immunoprecipitation with an antibody to LXRα and subsequent blotting with an antibody to Foxa2 shows a strong interaction between LXRα and Foxa2, in both GW and T09 treatment, but not in IgG and vehicle controls (right panel). (D) Heatmaps of Foxa2 and FXR ChIP-Seq at ATAC-Seq regions induced by GW4064 (60,416 regions, PeakSeq FDR 5%, q-value < 0.05; left panel) and Foxa2 and LXRα ChIP-Seq signal at ATAC-Seq regions induced by LXR ligands GW3965 and T09 (59,054 regions GW3965, 59,783 regions T09, FDR 5%, q-value < 0.05, middle, right panel). (E) Ligand-responsive binding of FXR and LXRα is absent in *Foxa2* mutants and is Foxa2-dependent. Heatmaps of FXR and Foxa2 ChIP-Seq signal at sites of FXR binding induced by GW4064 in wildtype controls (left panel) and absent in *Foxa2* mutants. Heatmaps of LXRα and Foxa2 ChIP-Seq signal at sites of LXRα binding induced by GW3965 (middle panel) and T09 (right panel) in wildtype controls and absent in *Foxa2* mutants.

(Supplemental Figure 3C). Hence, a decrease in LXRα binding in Foxa2 mutants is independent of LXRα expression.

Surprisingly, IR-1 and DR-4 motifs for FXR and LXR, respectively, were not overrepresented in scanning motif analysis in regions occupied by these factors in *Foxa2* mutants. Instead, motifs for PPAR receptors (DR-1 element) and other factors (AP-2, zinc fingers) were enriched in these targets (Supplemental Figure 3D). EnrichR analysis of bound regions in *Foxa2*-deficient livers identified highly enriched pathways — including "calcium signaling" and "G-protein signaling" — that were not found in nuclear receptor targets in wildtype controls (Supplemental Figure 3E).

3.5. Ligand-dependent activation of FXR and LXR gene expression is Foxa2-dependent

To test whether changes in chromatin accessibility and transcription factor binding have functional consequences, we performed RNA-Seq analysis in livers of *Foxa2* mutants and their control littermates were treated with FXR agonist. Expression of classical FXR targets (*Nr0b2* & Ostb/*Slc51b*) with ligand-independent binding was induced by the ligand in a *Foxa2*-independent manner. Also, mRNA levels of bile acid synthesizing enzymes *Cyp7a1* and *Cyp8b1* are repressed to the same extent in *Foxa2* mutants as in control littermates (Supplemental Figure 1C).

Then, we assessed the expression of FXR targets *Cyp3a11* and *Nr1i2;* because, an increase in chromatin accessibility induced at these loci during the ligand activation was absent in *Foxa2*-deficient livers and newly opened chromatin regions corresponded to additional, ligand-dependent Foxa2 binding (Figures 2B and 3C). While mRNA levels of both genes are increased by ligand treatment in wildtype controls, the increase is reduced in *Foxa2* mutants (Figure 5A). In addition, the expression of numerous Foxa2-dependent FXR target genes (induced by ligand in wild-type mice, but completely blunted in *Foxa2* mutants) activated by GW4064 is shown in the heatmap in Figure 5B. While GW4064 induced expression of 367 genes in wild-type mice, expression of 553 genes was changed in *Foxa2* mutants treated with this compound (Figure 5C, top panel). An overwhelming majority (420/554) were differentially expressed only in *Foxa2*-deficient mice. Overall, mRNA levels of 367 genes were differentially expressed in wild-type mice treated with GW4064, but only 133 showed comparable changes in *Foxa2* mutants. Hence, Foxa2 deficiency affects ligand-dependent activation of FXR gene expression in two ways: First, the expression of hundreds of genes induced by the ligand in wildtype controls is blunted in *Foxa2* mutants (Figure 5B); and then, mRNA levels of numerous genes that are not changed by the ligands in control mice are changed in *Foxa2*-deficient livers (Figure 5C).

Ingenuity pathway analysis (IPA) of differentially expressed transcripts in wildtype livers treated with FXR ligand identified activation of nuclear receptors pathways, including FXR, PXR, CAR, and LX (Figure 5D, left panel). In contrast, "hepatic cholestasis", "insulin receptor signaling", and "PPARα activation" were among the enriched pathways in *Foxa2* mutants treated with GW4064 (Figure 5D, right panel), consistent with previous phenotypic characterization [14,30]. Next, we employed computational network analysis to investigate which transcription factors mediated the gene expression changes observed in mice treated with FXR agonists. IPA network analysis identified FXR/RXR heterodimer and a network of FXR (*Nr1h4*) and closely related receptors PXR (*Nr1i2*) and CAR (*Nr1i3*) activating ligand-dependent gene expression in wildtype controls (Figure 5E). Interestingly, gene repression observed in *Foxa2* mutants treated with GW4064 is regulated by chromatin repressors, DNA methyltransferases Dmnt3a & Dnmt3b, and lysine histone demethylases Kdm5a & Kdm5b (Figure 5F).

We observed similar results in RNA-Seq analysis in livers of *Foxa2* mutants and their control littermates treated with LXR agonists. Expression of classical LXR targets (*Abca1*, *Abcg1*, *Abcg5*, *Abcg8*, *Srebf1*) with ligand-independent binding is induced by LXR agonists in a *Foxa2*-independent manner (Supplemental Figure 1C). For ligand-dependent LXR targets *Scd1* and *Lpin* — with an observed increase in chromatin accessibility absent in Foxa2-deficient livers (Figures 2B and 3C) — mRNA levels are induced by ligand treatment in wildtype controls, but not in *Foxa2* mutants (Figure 6A). Moreover, expression of numerous Foxa2-dependent LXRα target genes (increased by ligand in wild-type mice, but blunted in *Foxa2* mutants) activated either by GW (left panel) or T09 (right panel) is shown in heatmaps in Figure 6B. While GW induced expression of only 104 genes in wild-type mice, expression of 307 genes was changed in *Foxa2* mutants treated with this compound (Figure 6C, top panel). An overwhelming majority (267/307) were differentially expressed only in *Foxa2*-deficient mice. We observed a similar pattern in mice treated with T09. Overall, mRNA levels of 427 genes were differentially expressed in wild-type mice treated with T09, but only 195 showed comparable changes in *Foxa2* mutants (Figure 6C, bottom panel). Also, the deletion of *Foxa2* resulted in additional 217 genes that were not changed in controls, but differentially regulated in *Foxa2* mutants treated with T09 (Figure 6C, bottom panel). Hence, similar to FXR analysis, Foxa2 deficiency affects ligand-dependent activation of LXRα gene expression in two ways: First, the expression of hundreds of genes induced by the ligand in wildtype controls is blunted in *Foxa2* mutants (Figure 6B); and then, mRNA levels of numerous genes that are not changed by the ligands in control mice are changed in *Foxa2*-deficient livers (Figure 6C).

Ingenuity pathway analysis (IPA) of differentially expressed transcripts in wildtype livers treated with LXR ligands identified activation of nuclear receptors pathways, including LXR, FXR, PXR, and TR (Figure 6D, top panel). In contrast, "unfolded protein response", "protein ubiquitination", "PPARα activation", and "xenobiotic metabolism" were among the enriched pathways in *Foxa2* mutants treated with GW and T09 (Figure 6D, bottom panel). IPA network analysis identified networks regulated by LXRα(*Nr1h3*)/LXRβ(*Nr1h2*) and their target Srebf1 (Figure 6D, left panel) and Foxa2 to activate gene expression (Figure 6E, middle panel), while PPARα activity was downregulated in wildtype controls treated with LXR agonists (Figure 6E, right panel). In contrast, PPARα activity is upregulated in *Foxa2* mutants treated with T09 (Figure 6F, right panel). In addition, we observed that the endoplasmic reticulum stress network regulated by Atf6 and Xbp1 is upregulated in *Foxa2* mutants treated with GW3965 (Figure 6F right panel). We have previously reported that endoplasmic reticulum stress is induced in *Foxa2*-deficient mice during chronic activation of FXR with cholic acid [14]. We also noted that the activity of DNA methyltransferases Dnmt3a & Dnmt3b is induced, which leads to the repression of targets in *Foxa2* mutants during LXRα activation (Figure 6E, middle panel) and FXR activation (Figure 5F, left panel). Overall, changes in chromatin accessibility and transcription factor binding observed with the addition of FXR and LXR agonists lead to the activation of gene expression in wild-type controls that is inhibited in *Foxa2* mutants.

3.6. Foxa2 is required to enable ligand-dependent activation of the proper nuclear receptor

We observed that PPAR-bound DR-1 elements are highly enriched in regions with increased accessibility and PPARα targets were upregulated in *Foxa2* mutants treated with FXR and LXR agonists (Figures 5D and 6D, F, Supplemental Figure 2D). Based on these findings, we hypothesized that to enable ligand-dependent activation

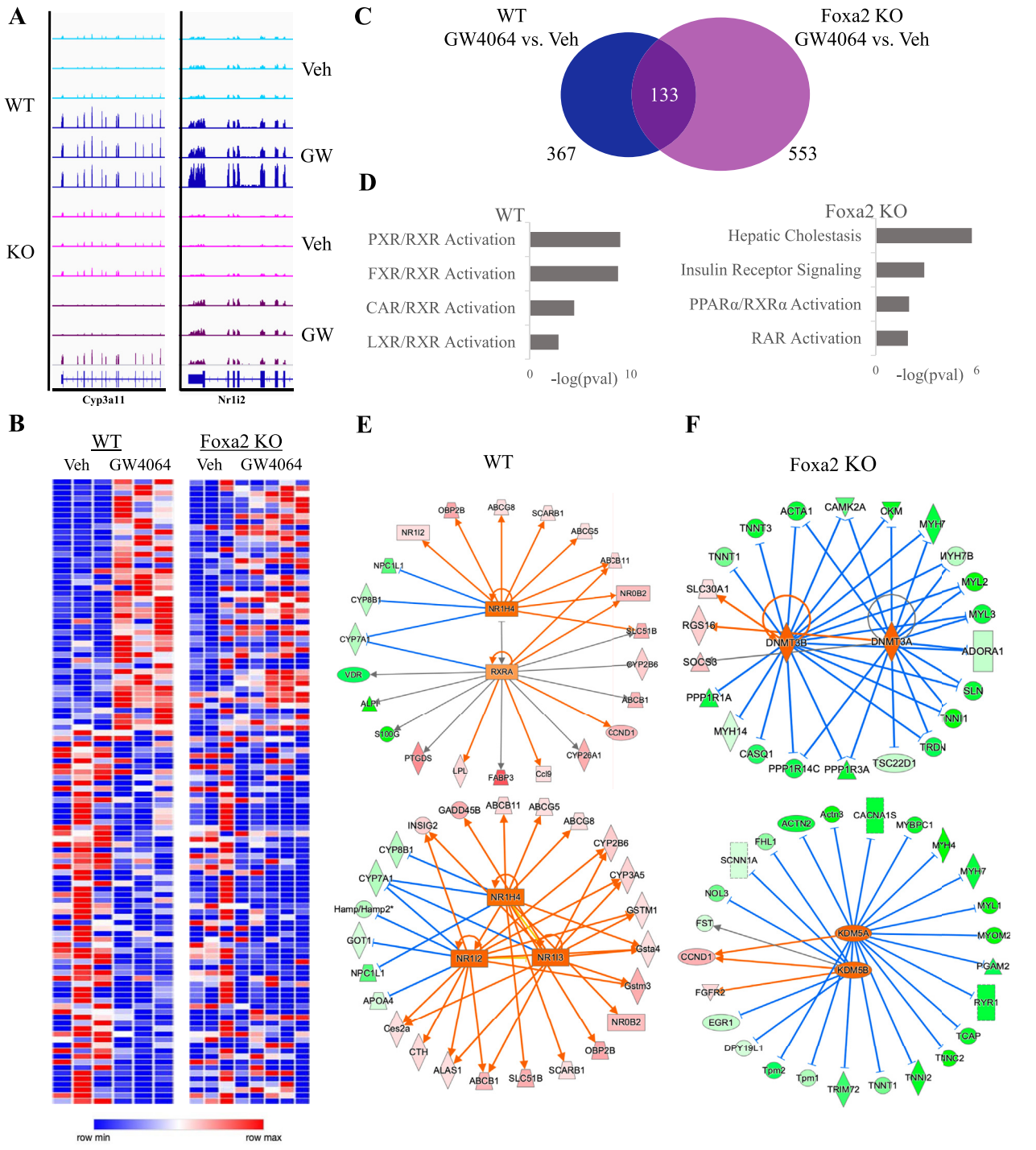

Figure 5: Ligand-dependent activation of FXR gene expression is Foxa2-dependent. (A) RNA-seq track view in IGV showing that ligand-responsive activation of Cyp3a11 (left panel) and Nr1i2 (right panel), well-known FXR targets, is Foxa2-dependent. (B) Heatmap (RNA-Seq gene expression) of Foxa2-dependent FXR targets activated or repressed by GW4064. Expression of 112 genes differentially expressed in livers of wild-type mice treated with GW4064, but not changed in Foxa2 mutants. (C) Venn diagram showing the number of differentially expressed genes with ligand activation by GW4064 (367 genes in WT, 553 genes in Foxa2 KO, 133 genes in common. Differential expression was analyzed using EdgeR (FDR 5%). (D) Ingenuity pathway analysis (IPA) of differentially expressed transcripts in wildtype livers treated with FXR ligand identified activation of nuclear receptors pathways, including FXR, PXR, CAR, and LXR (p-values $<$ 1.82E-9, 1.10E-9, 3.99E-5, and 0.0015, respectively, top panel). In contrast, "calcium signaling", "Type II diabetes", and "white adipose tissue browning" were among enriched pathways in *Foxa2* mutants treated with GW4064 (p-values $<$ 1.26E-12, 5.63E-5, 2.82E-4, and 0.0021, respectively, in bottom panel). (E) IPA network analysis identified FXR/RXR heterodimer and a network of FXR (*Nr1h4*) and closely related receptors PXR (*Nr1i2*) and CAR (*Nr1i3*) activating ligand-dependent gene expression in wildtype controls (blue line represents activation, orange line repression, and gray line the association with expression change). (F) Gene repression observed in *Foxa2* mutants treated with GW4064 is regulated by chromatin repressors, DNA methyltransferases Dnmt3a and Dnmt3b, and lysine histone demethylases Kdm5a and Kdm5b (blue line represents activation, orange line repression, and gray line the association with expression change).

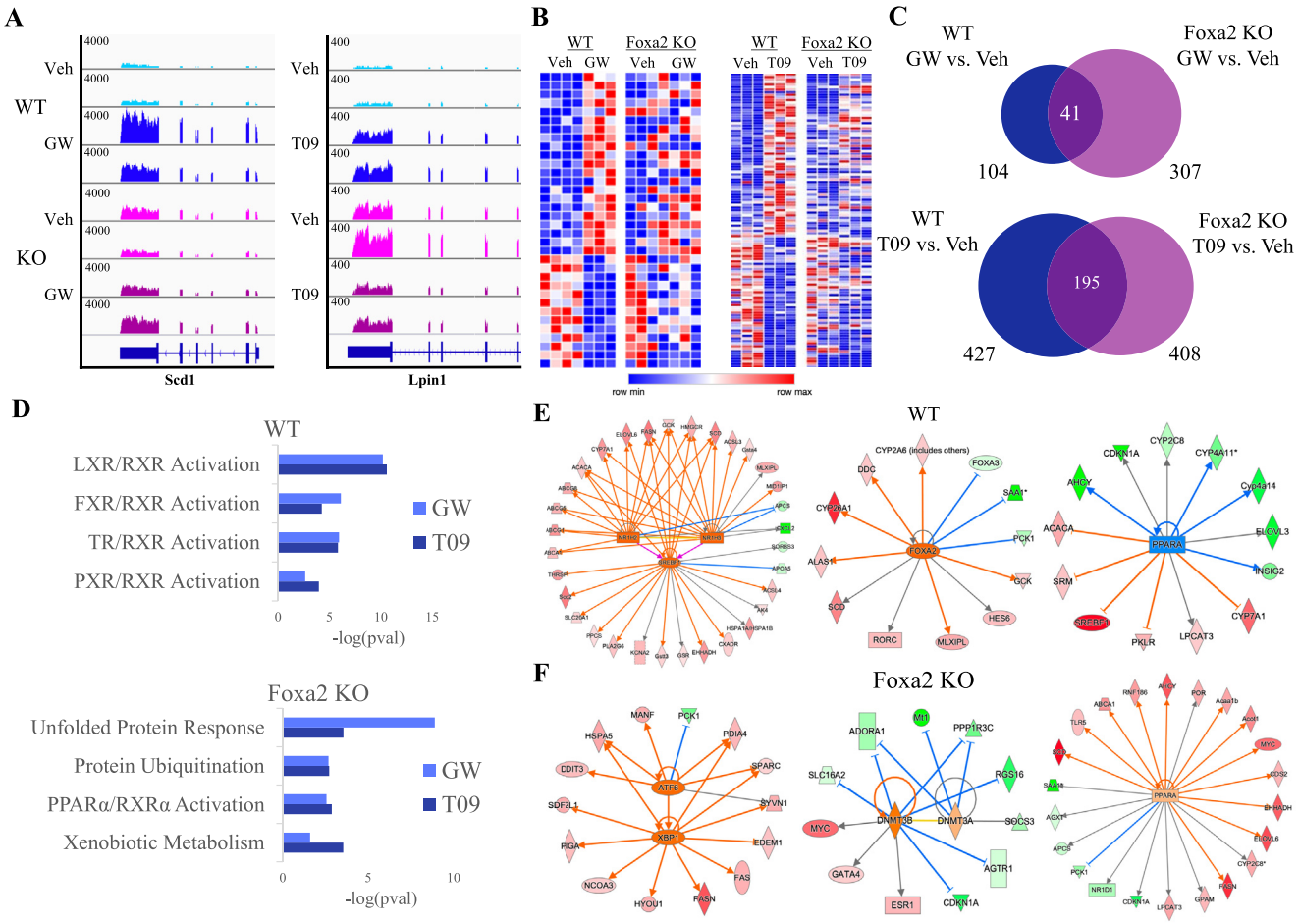

Figure 6: Ligand-dependent activation of LXRα gene expression is Foxa2-dependent. (A) RNA-seq track view in IGV showing that ligand-responsive activation of Scd1 (GW, left panel) and Lpin1 (T09, right panel), well-known LXRα targets, is Foxa2-dependent. (B) Heatmap (RNA-Seq gene expression) of Foxa2-dependent LXRα targets activated or repressed by agonists. Gene expression by LXR ligands (GW, 35 genes, left panel; T09, 116 genes, right panel; EdgeR, FDR < 5%) changed in wild-type mice, but not in Foxa2 mutants. (C) Venn diagram showing the number of differentially expressed genes with ligand activation by GW (top panel, 104 genes in WT, 307 genes in KO, 41 genes in common) and T09 (bottom, 427 genes in WT, 408 genes in KO, 195 genes in common). Differential expression was analyzed using EdgeR (FDR 5%). (D) Ingenuity pathway analysis (IPA) of differentially expressed transcripts in wildtype livers treated with LXR ligands identified activation of nuclear receptors pathways, including LXR, FXR, PXR, and TR (p-values < 6.31E-11 and 2.53E-11, 7.59E-7 and 5.50E-5, 1.13E-6 and 1.45E-6, 0.0023 and 0.00011, for GW and T09, respectively, top panel). In contrast, "unfolded protein response", "protein ubiquitination", "PPARα activation", and "xenobiotic metabolism" were among enriched pathways in *Foxa2* mutants treated with GW and T09 (p-values < 1.26E-9 and 0.00028, 0.0021 and 0.0019, 0.0028 and 0.0014, 0.025 and 0.00028, for GW and T09, respectively, bottom panel). (E) IPA network analysis identified networks regulated by LXRα(*Nr1h3*)/LXRβ(*Nr1h2*) and their target Srebf1 (left panel) and Foxa2 to activate gene expression (middle panel), while PPARα activity was downregulated in wildtype controls treated with LXR agonists (right panel) (blue line represents activation, orange line repression, and gray line the association with expression change). (F) We observe that the endoplasmic reticulum stress network, regulated by Atf6 and Xbp1 is upregulated in *Foxa2* mutants treated with GW3965 (right panel). We also observe that the activity of DNA methyltransferases Dnmt3a & Dnmt3b is induced, which leads to the repression of targets in Foxa2 mutants during LXRα activation (middle panel), similar to FXR activation (Figure 5F, left panel). PPARα activity is upregulated in *Foxa2* mutants treated with T09 (right panel), while we observe the opposite effect in wildtype control (Figure 5E, right panel) (blue line represents activation, orange line repression, and gray line the association with expression change).

of the proper nuclear receptor, binding of a competing receptor is repressed in wildtype conditions and activated in the absence of Foxa2. (Figure 7A). Hence, we performed PPARα ChIP-Seq in mice treated with FXR and LXR agonists and observed more significant binding in Foxa2 mutants treated with the ligand than in control littermates (GW4064: 1,979 regions WT, 2,667 KO; GW3965: 110 regions WT, 2,508 regions KO; T09 313 regions WT, 1813 KO; Figure 7B). In particular, there is almost no PPARα binding in wild-type mice treated with LXR ligands, while PPARα occupies about 2,000 sites in *Foxa2* mutants. Motif scanning analysis identified DR-1 elements bound by PPAR receptors, consensus sites for nuclear receptor half-site, and *forkhead* motif —highly enriched in regions bound by PPARα in Foxa2-deficient livers treated with FXR and LXR ligands (Figure 7C). In addition, sites bound by PPARα during ligand activation in *Foxa2* mutants overlap with regions occupied by FXR or LXR in wild-type mice in a ligand-independent manner (GW4064: 1149/2667; GW3975: 667/2508; T09: 516/1813; Figure 7D). Ligand-dependent binding of these receptors requires an increase in chromatin accessibility facilitated by Foxa2 and these sites remain closed in Foxa2 mutants.

In summary, our data show that in addition to ligand-independent sites (Figure 8A, top panel), FXR and LXRα bind to ligand-dependent NR sites that are inaccessible without ligand activation and become exposed upon stimulation. Pioneer factor Foxa2 enables ligand-dependent NR binding, evicting the nucleosome that occludes NR

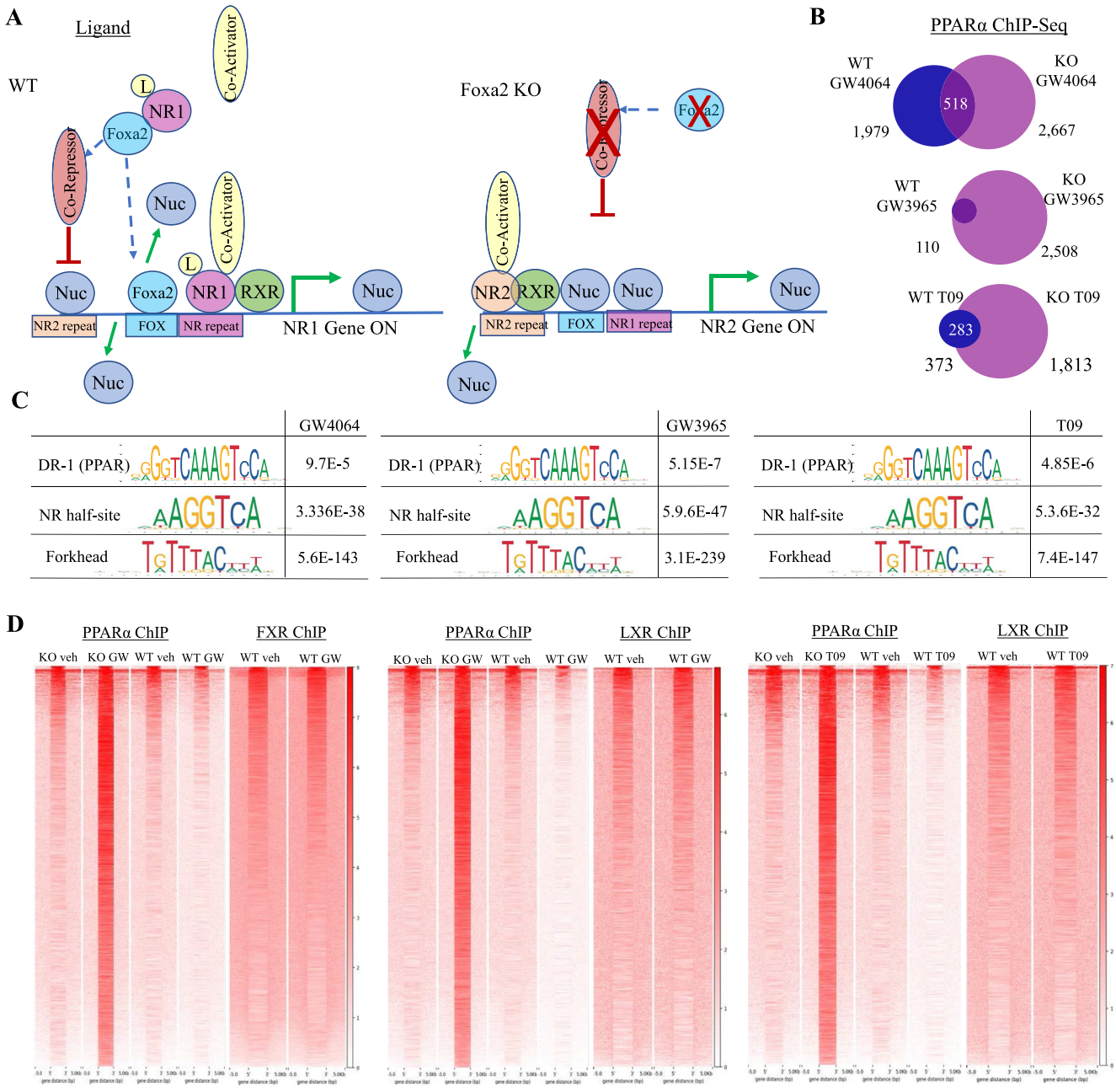

Figure 7: Foxa2 is required to enable ligand-dependent activation of the proper nuclear receptor. (A) We hypothesized that to enable ligand-dependent activation of the proper nuclear receptor, binding of a competing receptor is repressed in wildtype conditions and activated in the absence of Foxa2. (B) Venn diagrams showing PPARα binding is induced by FXR and LXR agonists in *Foxa2* mutants (GW4064: 1,979 regions WT, 2,667 KO; GW3965: 110 regions WT, 2,508 regions KO; T09 313 regions WT, 1813 KO; PeakSeq, FDR < 5%, q-value < 0.07 vs. Input control). (C) Scanning motif analysis identified DR-1 elements bound by PPAR receptors, consensus sites for nuclear receptor half-site, and *forkhead* motif as highly enriched in regions bound by PPARα in *Foxa2*-deficient livers treated with FXR and LXR ligands. (D) Sites bound by PPARα during ligand activation in *Foxa2* mutants overlap with regions occupied by FXR or LXR in wild-type mice in a ligand-independent manner (GW4064: 1149/2667; GW3975: 667/2508; T09: 516/1813). Heatmaps of PPARα and corresponding nuclear receptor (FXR or LXR) ChIP-Seq signal at sites bound by PPARα in *Foxa2* mutants (and not in wildtype controls) treated with a ligand (GW4064 left panel, GW3965 middle panel, T09 right panel).

binding site upon ligand activation. Two mechanisms are plausible: 1) Foxa2 is bound in the absence of ligand and evicts the nearby nucleosome occluding the nuclear receptor response element upon ligand binding (Figure 8A, middle panel); and 2) Foxa2 is not bound before ligand activation (Figure 8A, bottom panel). A dramatic change in Foxa2 occupancy observed in livers treated with FXR agonist GW4064, and LXR agonists GW3965 and T09 (Figure 3C), provides overwhelming evidence for the second mechanism.

More importantly, Foxa2 is required to achieve proper ligand-dependent activation of the receptor that binds the ligand in two ways. 1) Repressing activity of a competing receptor. We observed significantly more PPARα binding in *Foxa2* mutants treated with FXR and LXR ligands than in control littermates (Figure 7B). Also, "PPARα activation" pathway was significantly overrepresented in differentially expressed genes in *Foxa2* mutants during each ligand treatment (Figures 5D and 6D). With ligand addition, Foxa2 forms a complex with

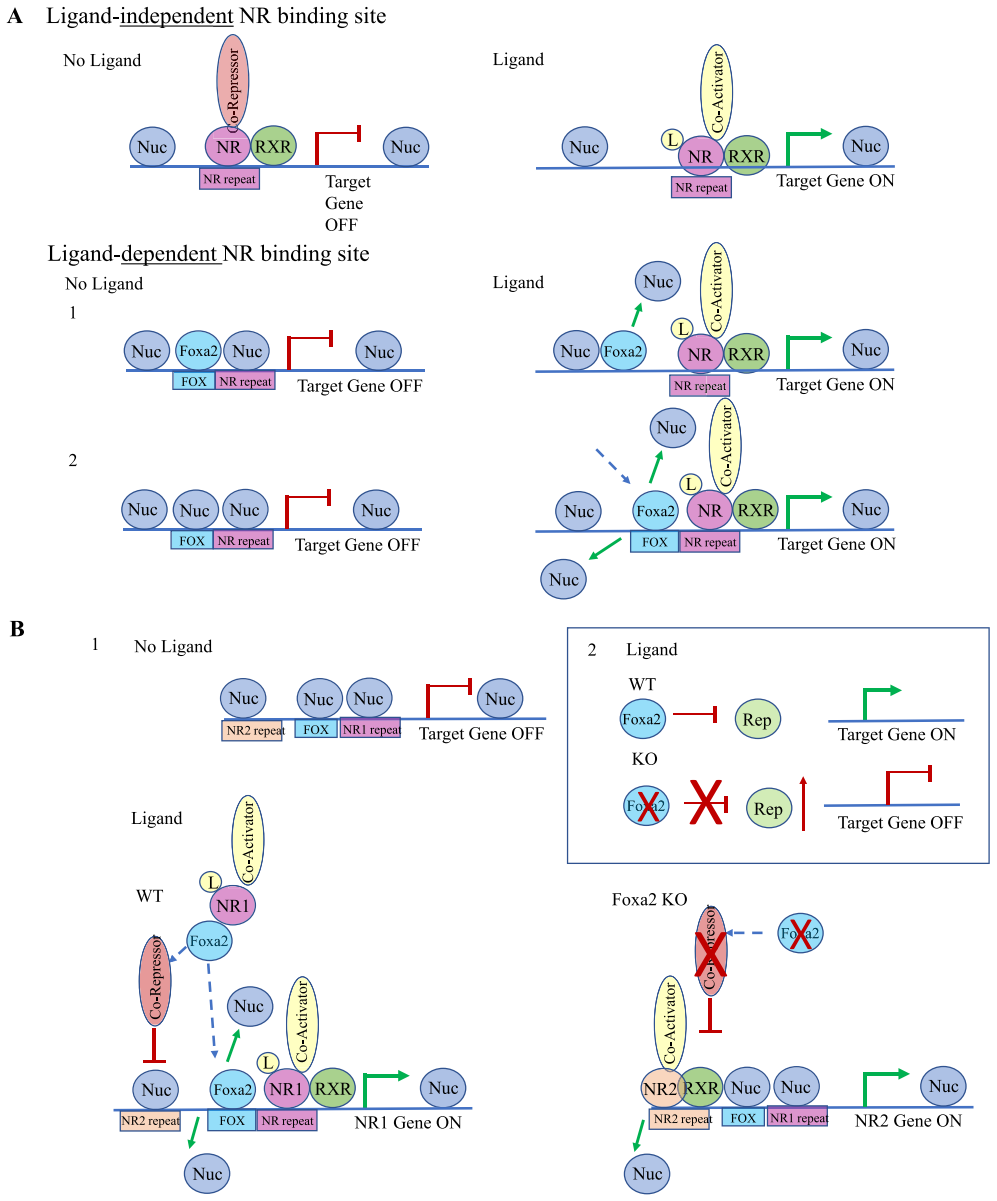

Figure 8: Model describing how Foxa2 enables ligand-dependent activation of LXRα. (A) We distinguish between ligand-independent and ligand-dependent nuclear receptor (NR) binding sites. Ligand-independent NR sites are always accessible and the mechanism of LXR activation is consistent with the classical model (top panel). In the absence of ligand, the receptor is bound to the DNA in complex with a co-repressor (top panel, left), while ligand binding induces a conformational change, co-repressor/co-activator exchange, and initiation of transcription (top panel, right). In contrast, ligand-dependent NR sites are inaccessible without ligand activation and become exposed upon stimulation (middle and bottom panel). We demonstrate that pioneer factor Foxa2 enables ligand-dependent NR binding, evicting the nucleosome (Nuc) that occludes NR binding site upon ligand activation. Two mechanisms are plausible: 1) Foxa2 is bound in absence of ligand and evicts the nearby nucleosome occluding NR response element upon ligand binding (middle panel showing a pre-existing Foxa2 binding site, increase in chromatin accessibility, and a new LXRα binding site upon agonist addition); 2) Foxa2 is not bound before ligand activation (bottom panel showing a novel ligand-dependent Foxa2 site corresponding to increase in chromatin accessibility and additional LXRα binding during ligand activation). (B) Foxa2 is required to achieve proper ligand-dependent activation of the receptor that binds that ligand in two ways: 1) Repressing activity of another receptor. In addition to the Foxa2 complex with the liganded nuclear receptor (NR1, such as LXRα) that opens previously inaccessible chromatin, allowing the additional binding of Foxa2 and the receptor; Foxa2 also represses other nuclear receptors (NR2, such as PPARα) from accessing nearby sites. In absence of Foxa2, the repression is lifted, allowing for NR2 binding and activation of its target genes, even though the mice are treated with a ligand NR1. 2) Activation of proper gene expression. During ligand activation, Foxa2 represses chromatin repressors, such as Kdm5a/b and Dnmt3a/b, and allows gene activation. The activity of these repressors is induced in Foxa2 mutants, leading to the repression of target genes.

the liganded nuclear receptor. That complex binds previously inaccessible chromatin by the pioneering activity of Foxa2 at the *forkhead* site. While Foxa2 facilitates activation of the proper nuclear receptor, it also represses competing nuclear receptors from accessing nearby sites. In the absence of Foxa2, the repression is lifted, allowing PPARα binding and activation of its target genes, even though the mice are treated with a ligand for a different receptor. (Figure 8B, bottom panel). 2) Activation of proper gene expression. During ligand activation, Foxa2 represses chromatin repressors Kdm5a/b and Dnmt3a/b, allowing for gene activation. The activity of these repressors is induced in Foxa2 mutants (Figures 5F and 6F), which leads to the repression of target genes (Figure 8B, top panel).

4. DISCUSSION

Our results challenge the classical paradigm of ligand-dependent activation of type II nuclear receptors, involving ligand-independent mechanism depending only on co-repressor/co-activator exchange that leads to the initiation of transcription upon ligand binding (Figures 1A and 8A). Unlike type I nuclear receptors, such as ER and AR which change their subcellular localization and translocate to the nucleus upon ligand binding, LXR and other type II nuclear receptors, including PPAR and FXR, are always nuclear; and hence, should be able to access their binding sites. However, we demonstrate that in acute 4-h activation, the binding of FXR and LXRα is dramatically induced and extensive chromatin accessibility changes observed on the addition of an agonist are because of Foxa2 evicting nucleosomes that enable subsequent FXR and LXRα binding to DNA. Our data agree with a previous study reporting that LXRα during different physiological conditions (chronic activation with 14 daily ligand injections) is largely ligand-dependent [8]. Furthermore, FXR ChIP-Seq in human hepatocytes identified twice as many sites occupied with GW4064 treatment (2759 for vehicle and 5235 for GW), suggesting that ligand-dependent FXR binding is conserved in humans [31].

Our model replacing the classical paradigm distinguishes between ligand-independent and ligand-dependent NR binding sites (Figure 8A). Classical FXR and LXRα targets (Nr0b2 and Ostb (*Slc51b*); Srebf1 and Abca1, Supplemental Figure 1B) bind DNA in a ligand-independent manner. Both binding and ligand-responsive gene expression of these targets is Foxa2-independent (Supplemental Figures 1B and C). In contrast, ligand-dependent binding is observed at most FXR and LXRα targets (Figures 1D and 4E). Both binding and activation of ligand-responsive gene expression of these targets depend on Foxa2 (Figures 4E, 5C, 6C). These results are consistent with our previous study which determined that ligand-responsive activation of FXR gene expression with cholic acid is Foxa2-dependent [13].

In addition, we determine a novel mechanism of nuclear receptor ligand-dependent binding. Foxa1, a close paralog of Foxa2, is required for the binding of steroid receptors ER and AR and hormone-dependent gene activation by these receptors [6,32]. While Foxa1 is bound before ligand activation of steroid receptors and their translocation to the nucleus [6,7,33,34], we found that Foxa2 occupancy is drastically induced by the activation of type II receptors FXR and LXRα; which suggests that there is an interdependent relationship between Foxa2 and nuclear receptor binding to DNA during ligand activation.

Ultimately, we have discovered a novel role for Foxa2, as a "gatekeeper" of ligand-dependent activation by the proper receptor, one that binds the added ligand. First, to achieve activation, Foxa2 inhibits the activity of chromatin repressors Dnmt3a/b and Kdm5a/b, leading to increased expression of their targets. In *Foxa2* mutants treated with FXR and LXR agonists, these repressors are no longer inhibited, leading to decreased expression of their targets. Subsequently, Foxa2 represses the activity of a competing receptor. PPARα gene expression is inhibited in wild-type mice treated with FXR and LXR agonists but activated in *Foxa2*-deficient mice upon receptor activation. Because nuclear receptors extensively share their binding sites, Foxa2 also facilitates binding and activation of gene expression of the proper nuclear receptor when the ligand is introduced while inhibiting access to competing factors. Considering that ligand-responsive activation of gene expression by both FXR and LXRα is Foxa2-dependent, it is likely that Foxa2 is required to modulate chromatin accessibility in a common mechanism mediating ligand-activation of all type II nuclear receptors.

5. CONCLUSIONS

Contrary to the accepted model, our data show that FXR and LXRα occupy both ligand-independent and ligand-dependent sites, which are inaccessible without the agonist. We found that pioneer factor Foxa2 opens chromatin for FXR and LXRα binding during acute ligand activation.

In addition, Foxa2 interacts with these receptors in a ligand-dependent manner. Furthermore, PPARα binding is induced in *Foxa2* mutants treated with FXR and LXR ligands, suggesting that Foxa2 restricts the activity of competing receptor PPARα to ensure ligand-dependent activation of proper receptors.

AUTHOR CONTRIBUTIONS

JK: Software, Formal Analysis, Data Curation, Writing - Review & Editing; XW: Methodology, Investigation, Writing - Review & Editing; NAR: Software, Formal Analysis, Data Curation, Writing - Review & Editing; AJP: Methodology, Software, Formal Analysis, Writing - Review & Editing; CW: Investigation, Writing - Review & Editing; IMB: Conceptualization, Formal Analysis, Investigation, Writing — original draft, Supervision, Project administration, Funding acquisition.

ACKNOWLEDGMENTS

We thank S. Srabani and J. Turner for the helpful comments and technical assistance. We thank S Anakk and I. Schulman for the critical reading of the article. All sequencing was performed at UVA Genome Analysis and Technology Core, RRID:SCR_018883. I.M.B. is supported by National Diabetes and Digestive and Kidney Diseases Institute R01 award DK121059.

CONFLICT OF INTEREST

Authors declare no competing interests.

APPENDIX A. SUPPLEMENTARY DATA

Supplementary data to this article can be found online at https://doi.org/10.1016/j.molmet.2021.101291.

REFERENCES

[1] Kidani, Y., Bensinger, S.J., 2012. Liver X receptor and peroxisome proliferator-activated receptor as integrators of lipid homeostasis and immunity. Immunological Reviews 249(1):72—83.

[2] Lin, C.Y., Gustafsson, J.A., 2015. Targeting liver X receptors in cancer therapeutics. Nature Reviews Cancer 15(4):216—224.

[3] Schaap, F.G., Trauner, M., Jansen, P.L., 2014. Bile acid receptors as targets for drug development. Nature Reviews Gastroenterology & Hepatology 11(1): 55—67.

[4] Schulman, I.G., 2010. Nuclear receptors as drug targets for metabolic disease. Advanced Drug Delivery Reviews 62(13):1307—1315.

[5] Wright, M.B., Bortolini, M., Tadayyon, M., Bopst, M., 2014. Minireview: challenges and opportunities in development of PPAR agonists. Molecular Endocrinology 28(11):1756—1768.

[6] Carroll, J.S., Liu, X.S., Brodsky, A.S., Li, W., Meyer, C.A., Szary, A.J., et al., 2005. Chromosome-wide mapping of estrogen receptor binding reveals long-range regulation requiring the forkhead protein FoxA1. Cell 122(1):33—43.

[7] Lupien, M., Eeckhoute, J., Meyer, C.A., Wang, Q., Zhang, Y., Li, W., et al., 2008. FoxA1 translates epigenetic signatures into enhancer-driven lineage-specific transcription. Cell 132(6):958—970.

[8] Boergesen, M., Pedersen, T.A., Gross, B., van Heeringen, S.J., Hagenbeek, D., Bindesboll, C., et al., 2012. Genome-wide profiling of liver X receptor, retinoid X receptor, and peroxisome proliferator-activated receptor alpha in mouse liver reveals extensive sharing of binding sites. Molecular and Cellular Biology 32(4):852–867.

[9] Friedman, J.R., Kaestner, K.H., 2006. The Foxa family of transcription factors in development and metabolism. Cellular and Molecular Life Sciences 63(19–20):2317–2328.

[10] Zaret, K.S., Carroll, J.S., 2011. Pioneer transcription factors: establishing competence for gene expression. Genes & Development 25(21):2227–2241.

[11] Li, Z., Schug, J., Tuteja, G., White, P., Kaestner, K.H., 2011. The nucleosome map of the mammalian liver. Nature Structural & Molecular Biology 18(6): 742–746.

[12] Li, Z., Gadue, P., Chen, K., Jiao, Y., Tuteja, G., Schug, J., et al., 2012. Foxa2 and H2A.Z mediate nucleosome depletion during embryonic stem cell differentiation. Cell 151(7):1608–1616.

[13] Bochkis, I.M., Schug, J., Rubins, N.E., Chopra, A.R., O'Malley, B.W., Kaestner, K.H., 2009 Jul 9. Foxa2-Dependent hepatic gene regulatory networks depend on physiological state. Physiological Genomics 38(2):186–195.

[14] Bochkis, I.M., Rubins, N.E., White, P., Furth, E.E., Friedman, J.R., Kaestner, K.H., 2008. Hepatocyte-specific ablation of Foxa2 alters bile acid homeostasis and results in endoplasmic reticulum stress. Nature Medicine 14(8):828–836.

[15] Bochkis, I.M., Przybylski, D., Chen, J., Regev, A., 2014. Changes in nucleosome occupancy associated with metabolic alterations in aged mammalian liver. Cell Rep 9(3):996–1006.

[16] Zhang, L., Rubins, N.E., Ahima, R.S., Greenbaum, L.E., Kaestner, K.H., 2005. Foxa2 integrates the transcriptional response of the hepatocyte to fasting. Cell Metabolism 2(2):141–148.

[17] Buenrostro, J.D., Giresi, P.G., Zaba, L.C., Chang, H.Y., Greenleaf, W.J., 2013. Transposition of native chromatin for fast and sensitive epigenomic profiling of open chromatin, DNA-binding proteins and nucleosome position. Nature Methods 10(12):1213–1218.

[18] Whitton, H., Singh, L.N., Patrick, M.A., Price, A.J., Osorio, F.G., Lopez-Otin, C., et al., 2018. Changes at the nuclear lamina alter binding of pioneer factor Foxa2 in aged liver. Aging Cell 17(3):e12742.

[19] Price, A.J., Manjegowda, M.C., Kain, J., Anandh, S., Bochkis, I.M., 2020. Hdac3, Setdb1, and Kap1 mark H3K9me3/H3K14ac bivalent regions in young and aged liver. Aging Cell 19(2):e13092.

[20] Li, H., Durbin, R., 2009. Fast and accurate short read alignment with Burrows-Wheeler transform. Bioinformatics 25(14):1754–1760.

[21] Rozowsky, J., Euskirchen, G., Auerbach, R.K., Zhang, Z.D., Gibson, T., Bjornson, R., et al., 2009. PeakSeq enables systematic scoring of ChIP-seq experiments relative to controls. Nature Biotechnology 27(1):66–75.

[22] Dobin, A., Davis, C.A., Schlesinger, F., Drenkow, J., Zaleski, C., Jha, S., et al., 2013. STAR: ultrafast universal RNA-seq aligner. Bioinformatics 29(1):15–21.

[23] Li, B., Dewey, C.N., 2011. RSEM: accurate transcript quantification from RNA-Seq data with or without a reference genome. BMC Bioinformatics 12:323.

[24] Robinson, M.D., McCarthy, D.J., Smyth, G.K., 2010. edgeR: a Bioconductor package for differential expression analysis of digital gene expression data. Bioinformatics 26(1):139–140.

[25] Ramirez, F., Dundar, F., Diehl, S., Gruning, B.A., Manke, T., 2014. deepTools: a flexible platform for exploring deep-sequencing data. Nucleic Acids Research 42:W187–W191 (Web Server issue).

[26] Kuleshov, M.V., Jones, M.R., Rouillard, A.D., Fernandez, N.F., Duan, Q., Wang, Z., et al., 2016. Enrichr: a comprehensive gene set enrichment analysis web server 2016 update. Nucleic Acids Research 44(W1):W90–W97.

[27] Zambelli, F., Pesole, G., Pavesi, G., 2013. PscanChIP: finding over-represented transcription factor-binding site motifs and their correlations in sequences from ChIP-Seq experiments. Nucleic Acids Research 41:W535–W543 (Web Server issue).

[28] Yoshikawa, T., Shimano, H., Amemiya-Kudo, M., Yahagi, N., Hasty, A.H., Matsuzaka, T., et al., 2001. Identification of liver X receptor-retinoid X receptor as an activator of the sterol regulatory element-binding protein 1c gene promoter. Molecular and Cellular Biology 21(9):2991–3000.

[29] Lu, T.T., Makishima, M., Repa, J.J., Schoonjans, K., Kerr, T.A., Auwerx, J., et al., 2000. Molecular basis for feedback regulation of bile acid synthesis by nuclear receptors. Molecular Cell 6(3):507–515.

[30] Bochkis, I.M., Shin, S., Kaestner, K.H., 2013. Bile acid-induced inflammatory signaling in mice lacking Foxa2 in the liver leads to activation of mTOR and age-onset obesity. Molecular Metabolism 2(4):447–456.

[31] Zhan, L., Liu, H.X., Fang, Y., Kong, B., He, Y., Zhong, X.B., et al., 2014. Genome-wide binding and transcriptome analysis of human farnesoid X receptor in primary human hepatocytes, 1932-6203 (Electronic).

[32] Sahu, G., Wang, D., Chen, C.B., Zhurkin, V.B., Harrington, R.E., Appella, E., et al., 2010. p53 binding to nucleosomal DNA depends on the rotational positioning of DNA response element. Journal of Biological Chemistry 285(2):1321–1332.

[33] Hurtado, A., Holmes, K.A., Ross-Innes, C.S., Schmidt, D., Carroll, J.S., 2011. FOXA1 is a key determinant of estrogen receptor function and endocrine response. Nature Genetics 43(1):27–33.

[34] Glont, S.E., Chernukhin, I., Carroll, J.S., 2019. Comprehensive genomic analysis reveals that the pioneering function of FOXA1 is independent of hormonal signaling. Cell Reports 26(10):2558–2565 e3.

